Electron structure of TiO$_2$ composite films with noble metal nanoparticles

T.O. Busko[1], M.P. Kulish[1], O.P. Dmytrenko[1], N.V. Vityuk[2], A.M. Eremenko[2]
[1]Taras Shevchenko Kyiv National University,
64, Volodymyrska str., 01601 Kyiv, Ukraine;
E-mail: tbusko@gmail.com
[2]O.O. Chuiko Institute of Surface Chemistry, NAS of Ukraine,
17, General Naumov str., 03164 Kyiv, Ukraine

Abstract. Thin nanocrystalline films of TiO$_2$, TiO$_2$/ZrO$_2$, TiO$_2$/ZrO$_2$/SiO$_2$, TiO$_2$/ZrO$_2$/SiO$_2$/Ag and TiO$_2$/ZrO$_2$/SiO$_2$/Au were prepared using the sol-gel synthesis method. In this paper, we determined the bandgap for direct and indirect band-to-band transitions. Optical conductivity of the films was determined using the spectral ellipsometry method. Depending on the nanocomposite composition, optical conductivity is of different character due to light absorption caused by the presence of the structure intrinsic defects: oxygen vacancies (F^{2+}, F, and F$^+$ centers), Ti^{3+} ions and interstitial Ti atoms. Rearrangement of the electron spectrum in these thin films due to the aforementioned defects can improve photocatalytic activity in the UV and visible spectral ranges.

Keywords: anatase, nanocrystalline TiO$_2$ thin films, spectral ellipsometry, optical conductivity.

1. Introduction

Due to its activity in the UV spectral range, notable thermal and chemical stability, titanium dioxide is a promising material for creating devices for solar energetics, photocatalysts, protective coatings for spacecrafts, biologically active materials [1-5]. An important task for raising the efficiency of the photocatalyst is to improve the photoactivity of TiO$_2$ films and their composites in the visible spectral range.

Broadening the functional area of titanium dioxide can be achieved via its sensibilization to visible light. Advanced photocatalytic activity as well as mechanical, chemical and thermal stability of TiO$_2$ are known to be achieved by combining it with ZrO$_2$ and SiO$_2$ oxides [6-8]. Adding oxides of zirconium, aluminum, silicon to TiO$_2$ increases the specific area during the annealing of samples due to retardation of material sintering and prevention of phase transfer of anatase to less photoactive rutile [9, 10]. Mixed oxides appear to be more active because of formation of new active surface centers. This is caused by the change in recombination speed of charges and electron transfer at the boundaries of separated phases [11].

Nanoparticles of semiconductors modified by noble metals also exhibit high photocatalytic efficiency in photoprocesses. Noble metals, such as Pd, Pt, Au, Ag, applied to the oxide surface as films or introduced into TiO$_2$ matrix as nanoparticles, exhibit a high value of the Schottky barrier and thus act as electron traps. This reinforces the photogenerated electron-hole pair separation and electron transfer in interphase processes [12].

To determine the mechanism of photocatalysis involving pure nanosized TiO_2 and its nanocomposites, namely: the binary films of TiO_2/ZrO_2, ternary films of $TiO_2/ZrO_2/SiO_2$ and ternary films of $TiO_2/ZrO_2/SiO_2$ with embedded silver and gold nanoparticles, the authors of this paper studied optical absorption, determined bandgap widths and analyzed the optical conductivity spectra of the films in detail to ascertain their internal defect structure transformation and studied its impact on the optical properties of nanocomposites based on titanium dioxide.

2. Experimental

For the following study, non-porous films of TiO_2 were synthesized via the sol-gel method by using titanium tetraisopropoxide $Ti(OPr)_4$ as a source of Ti and acetylacetone (AcAc) as a complex former to decelerate the hydrolysis of Ti alkoxide. The molar ratio of the components in reaction mixture used to prepare the films was as follows: $Ti(OPr)_4$:AcAc:H_2O:C_2H_5OH = 1:0.87:3.45:48. To synthesize the films of TiO_2/ZrO_2 and $TiO_2/ZrO_2/SiO_2$ (49:21:30 mol.%), we used joint hydrolysis of titanium tetraisopropoxide and zirconium with tetraethoxysilane ($Ti(OC_3H_7)_4$, 97% $Zr(OC_3H_7)_4$, 70% Si $(OC_2H_5)_4$, 98% Aldrich) in the presence of acetylacetone (AcAc, 9% Aldrich) as a complex former and HCl as a stabilizer. To synthesize the films of $TiO_2/ZrO_2/SiO_2$/Ag (5 mol.%) and $TiO_2/ZrO_2/SiO_2$/Au (3.4 mol.%) with silver and gold nanoparticles, respectively, we added chloroauric acid ($HAuCl_4$ $3H_2O$, 99.9%, Aldrich) or silver nitrate ($AgNO_3$) to the $TiO_2/ZrO_2/SiO_2$ sol after prehydrolysis. Thus we obtained a film precursor to be applied onto the preliminarily cleared substrates. The films were applied by dip-coating with the extraction speed 1.5 mm/s. Once applied, the films were hydrolyzed in open air for 2 hours and heated in a muffler at 500 °C (4 hours). The rate of heating was 2 degrees/min.

Diffuse reflection spectra of the synthesized films were registered using a Perkin-Elmer Lambda Bio 35 spectrophotometer with a Labsphere RSA-PR-20 integrating sphere within the wavelength range 200–1000 nm. Extinction spectra were measured from the respective reflection spectra by using the Kubelka-Munk formula. Optical conductivity spectra of the films were measured using the spectral ellipsometry method. The experiment was carried out at room temperature within the energy range 1 to 5 eV at the angle of light incidence 72°.

3. Results and discussion

The XRD studies showed [13] that in the TiO_2 films obtained under specified conditions, a nanocrystalline anatase phase which persists for the TiO_2/ZrO_2 nanocomposites is formed. In the $TiO_2/ZrO_2/SiO_2$ triple compounds, an amorphous phase with the inclusions of crystalline TiO_2 prevails. When combining titanium dioxide with other oxides and metal nanoparticles, the optical conductivity in TiO_2, TiO_2/ZrO_2 and $TiO_2/ZrO_2/SiO_2$ differs. For the binary and ternary systems, the edge of the absorption band has a more pronounced gentle slope, in contrast to the individual TiO_2 (Fig. 1). This indicates formation of bonds ($Ti-O-Si$, $Ti-O-Zr$, $Si-O-Zr$) and the influence of ZrO_2 and SiO_2 on the size of nanoparticles of titanium dioxide [2], which results in the change in energy states that correspond to optical transitions in TiO_2. For $TiO_2/ZrO_2/SiO_2$/3.4% Au film (Fig. 1), we observe a low-intensity band of surface plasmon resonance (SPR) of gold nanoparticles with the peak at 2.25 eV. For the ternary film modified with silver nanoparticles, the SPR band that is characteristic for metallic silver nanoparticles at 400 nm was not observed. The lack of associated color can be explained by formation of the oxide shell around the core of silver nanoparticle.

Optical absorption for TiO_2/ZrO_2 nanocomposite observed at 2.5–3.5 eV leads to an increase of the absorption coefficient in this range. The absorption coefficient α is related to the bandgap width E_g of semiconductors as follows:

$$A(h\nu - E_g)^r = \alpha h\nu,$$

where $h\nu$ is the photon energy, A is a constant, $r = 2$ for indirect transitions, $r = 1/2$ for direct transitions. Bandgap width of anatase films was determined by the intersection of the $(\alpha h\nu)^{1/r}$ tangent to the photon energy axis. Monocrystalline titanium dioxide is semiconductor, the bandgap of which is determined from indirect transitions, however nanostructural materials based on it can also exhibit properties of direct semiconductors. Taking into account that the nature of the band-to-band transitions for these nanocrystalline films is unknown, we determined the bandgap width for two types of transitions: direct (E_{gd}) and indirect (E_{gi}) ones, Figs 2 and 3, respectively.
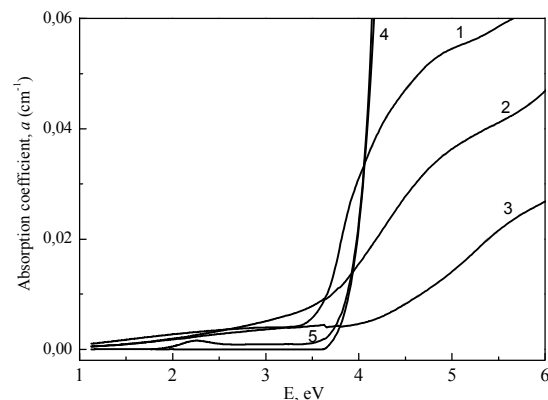
Fig. 1. Optical absorption spectra: *1* – TiO_2, *2* – TiO_2/ZrO_2, *3* – $TiO_2/ZrO_2/SiO_2$, *4* – $TiO_2/ZrO_2/SiO_2$/5% Ag, *5* – $TiO_2/ZrO_2/SiO_2$/3.4% Au.

Table 1. Values of the optical bandgaps E_{gi} and E_{gd} for TiO$_2$-based nanocomposites.

| Film	E_{gi}, eV	E_{gd}, eV
TiO$_2$	3.2	3.7
TiO$_2$/ZrO$_2$	2.9	4.2
TiO$_2$/ZrO$_2$/SiO$_2$	3.3	4.9
TiO$_2$/ZrO$_2$/SiO$_2$/Ag	3.6	4.2
TiO$_2$/ZrO$_2$/SiO$_2$/Au	3.6	4.2

Table 1 gives the values of the optical bandgaps E_{gi} and E_{gd} for TiO$_2$-based nanocomposites.

Table 1 shows that for the pure TiO$_2$ film in the case of indirect transitions, the obtained value is $E_{gi} = 3.2$ eV, which agrees well with the value of the bandgap width for anatase [14]. Like to the bulk samples of TiO$_2$, the films also display an indirect transition between the energy states O2p in the valence band and Ti3d in the conduction band. The value $E_{gd} = 3.7$ eV obtained for the films is overestimated and, therefore, it probably corresponds to one of the direct transitions typical for anatase.

For TiO$_2$/ZrO$_2$ film in the case of indirect transition, the obtained value is $E_{gi} = 2.9$ eV, which is smaller than the bandgap width of TiO$_2$ film. We can assume that this decrease of E_{gi} is due to formation of the surface localized energy states at the bottom of the conduction band as a result of the interface appearing between the TiO$_2$ and ZrO$_2$ nanoparticles. The value $E_{gd} = 4.2$ eV for this film is clearly overestimated for the bandgap width of TiO$_2$ nanoparticles.

In the case of the ternary TiO$_2$/ZrO$_2$/SiO$_2$ nanocomposites, the amount of interfaces between TiO$_2$ and ZrO$_2$ nanoparticles decreases, while the bandgap width $E_{gi} = 3.3$ eV increases as compared to its value for TiO$_2$/ZrO$_2$. Like to the TiO$_2$/ZrO$_2$ nanocomposite, the
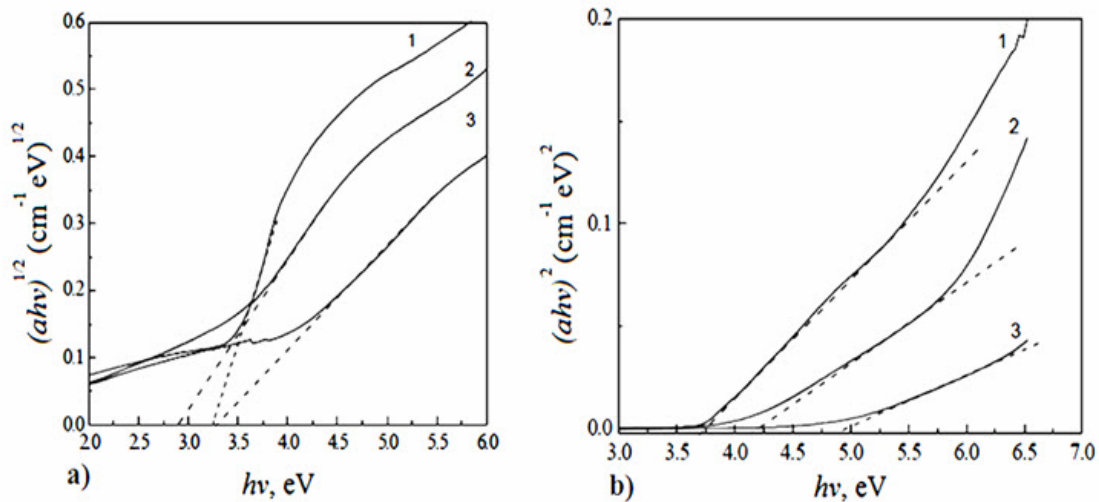
Fig. 2. Bandgap widths E_{gi} for indirect (*a*) and E_{gd} for direct (*b*) transitions in nanocomposites of TiO$_2$ (*1*), TiO$_2$/ZrO$_2$ (*2*), TiO$_2$/ZrO$_2$/SiO$_2$ (*3*).
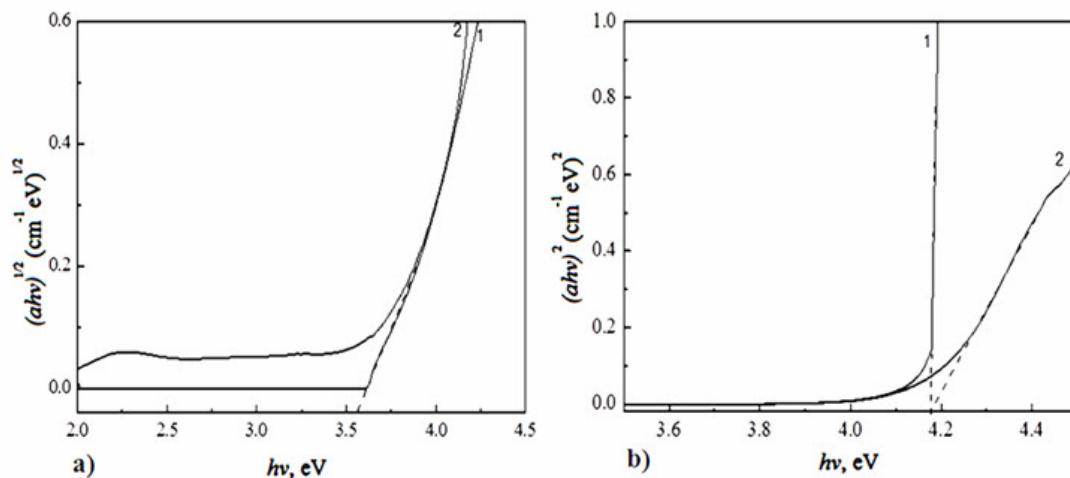
Fig. 3. Bandgap widths E_{gi} for indirect (*a*) and E_{gd} for direct (*b*) transitions in nanocomposites of TiO$_2$/ZrO$_2$/SiO$_2$/Ag (*1*), TiO$_2$/ZrO$_2$/SiO$_2$/Au (*2*).

value $E_{gd} = 4.9$ eV is clearly overestimated. With the introduction of Ag and Au nanoparticles into the ternary $TiO_2/ZrO_2/SiO_2$ nanocomposites, for both systems the E_{gi} value increases up to 3.6 eV, E_{gd} – up to 4.2 eV. It is possible that the increase of the bandgap width observed in the ternary nanocomposites and in films with noble metal nanoparticles is related with the quantum-size limitations of excitons that are manifested when decreasing the TiO_2 crystallite sizes due to the presence of SiO_2 oxides and Ag and Au metal nanoparticles [2, 12, 15].

Thus, considering that the bandgap of TiO_2 in the presence of oxides and metal nanoparticles increases, we can argue that the size of nanoparticles decreases respectively. In particular, this is due to the fact that at thermal treatment there is diffusion of metal atoms from the bulk to the film surface, when the concentration of metal atoms in the surface area becomes significant. This leads to deceleration of the anatase grain growth [16].

It is worth noting that for TiO_2 nanoparticles, there is not only an indirect band-to-band $\Gamma_3 \rightarrow X_{1b}$ transition that determines the width of the bandgap E_g, but also direct transitions with the energies exceeding its value [14], which is observed in optical extinction behavior.

It should also be noted that the presence of oxygen vacancies, Ti^{3+} ions and interstitial Ti atoms in TiO_2 along with the existence of surface states can lead to changes in the energy structure of titanium dioxide [3, 17]. These changes may partly affect the energy spectra of the valence and conduction bands, but primarily they have to manifest themselves in formation of additional acceptor and donor levels within the bandgap that correspond to deep and shallow charge carrier traps. The presence of these traps affects not only the broadening of the optical absorption region up to the visible range, but also leads to changes in radiative and nonradiative recombination of photogenerated charge carriers. This, in its turn, affects the photocatalytic activity of the TiO_2 surface [17].

The study of oxygen adsorption shows that intensities of individual bands change in different ways, which indicates a different nature of the defects. The analysis of the UV photoelectron spectroscopy results shows that the presence of these defects in the films is accompanied by a significant increase in the electron density of states and appearance of maxima with the energies at 1.17, 2.55, 2.81, and 2.0 eV [18]. The first three values are attributed to oxygen vacancies that can create three types of F centers: without trapping F^{2+} electrons, trapping one F^+ electron and trapping two F electrons. The energy levels that correspond to F and F^+ are occupied by electrons, and therefore they can act as color centers. The band at 2.0 eV is attributed to formation of Ti^{3+} impurity centers [3, 19]. At the same time in tetrahedral (i_m(Ti)) and octahedral (i_o(Ti)) pores of the tetragonal lattice of TiO_2 anatase, there can possibly exist interstitial Ti atoms that create additional energy states in the bandgap of TiO_2[17].
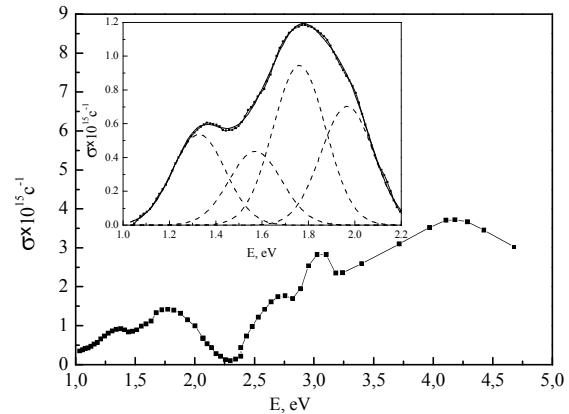
Fig. 4. Spectral dependence of optical conductivity $\sigma(E)$ for the TiO_2 film. (The insert shows the decomposition of $\sigma(E)$ into Gaussian components within the range 1.0–2.2 eV.)

In addition, in optical conductivity spectra $\sigma(E)$ in the range over 3.0 eV, there appear bands that correspond to optical transitions between different points of the Brillouin zone. For TiO_2 film, Fig. 4, the first of these transitions at the energy 3.1 eV relates to the fundamental absorption edge that defines the width of the bandgap E_{gi} in TiO_2 film and corresponds to the indirect band-to-band transition $\Gamma_3 \rightarrow X_{1b}$[14].

As seen in Fig. 4, within the bandgap of TiO_2 film at the energy 1.3 eV, there is a band that, according to the ultraviolet photoelectron spectroscopy study [19], can be attributed to absorption by F^{2+} centers. At the energies 1.57 and 1.75 eV, there are two extrema that are supposedly associated with donor levels arising due to the presence of interstitial Ti atoms in tetrahedral (i_m(Ti)) and octahedral (i_o(Ti)) pores of the tetragonal lattice in TiO_2 anatase, respectively [17]. At the energy 1.95 eV, there is an extremum that corresponds to absorption of Ti^{3+}ions [19]. The extremum at the energy 2.7 eV can be attributed to the presence of oxygen vacancies in TiO_x oxide of non-stoichiometric composition. These vacancies correspond to the F color centers [3, 19].

For the binary TiO_2/ZrO_2 film (Fig. 5) in the optical conductivity spectrum $\sigma(E)$, there are extrema at 1.25 and 1.82 eV that correspond to absorption caused by the presence of F^{2+} centers and Ti interstitial atoms in tetrahedral (i_m(Ti)) pores, respectively. The absorption band at the energy 2.1 eV indicates the presence of Ti^{3+} ions.

In the binary TiO_2/ZrO_2 film, unlike the individual TiO_2 film, new centers of absorption appearing at 2.55 eV are associated with F^+ centers (Fig. 5). In the case of TiO_2/ZrO_2, the absorption band at 2.85 eV is caused by the indirect band-to-band transition $\Gamma_3 \rightarrow X_{1b}$ that matches the width of the bandgap. This result agrees with the E_{gi} value 2.9 eV obtained from the optical extinction data, and can be attributed to the emergence of surface states in the given composite. It can be seen that due to the low density of states in these surface
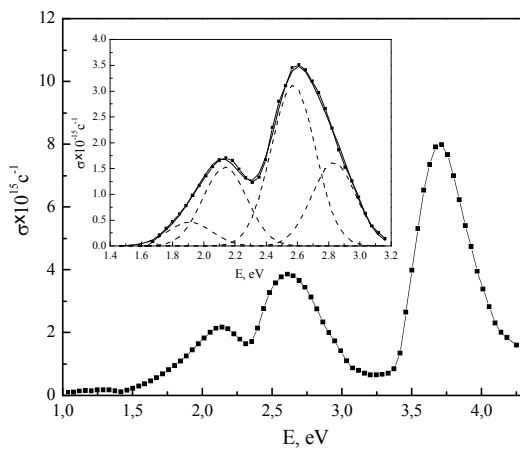
levels, the indicated absorption band intensity is negligible. The next absorption band is observed at the energy 3.8 eV and is rather indicative of the direct transitions in TiO_2.

In the case of triple $TiO_2/ZrO_2/SiO_2$ film, the maxima of the absorption bands associated with F^{2+} and F centers are located at 1.2 and 2.7 eV, respectively (Fig. 6).
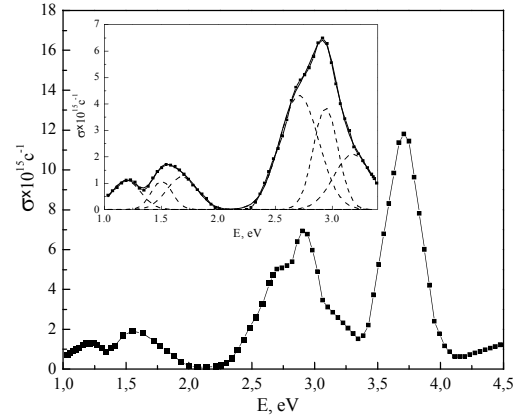
Unlike the binary films, in the optical conductivity spectrum of the ternary film, an extremum appears at 1.5 eV, which corresponds to the presence of interstitial atoms in octahedral (i_o(Ti)) pores. The absorption band caused by the presence of Ti^{3+} ions shifts toward lower energies and appears at 1.7 eV. It is possible that the optical conductivity $\sigma(E)$ maximum at 2.9 eV for the triple film is also caused by the presence of surface states at the bottom of the conduction band of TiO_2.

Remarkably, for the triple film, behavior of the spectral dependence $\sigma(E)$ also varies significantly within the energy range above 3.0 eV. We can assume that these changes are due to formation of new bonds between oxygen and Zr, Si via their replacement of Ti^{4+} ions, which eventually leads to a shift of the energy levels Γ_3 and X_{1b} in TiO_2. This, in its turn, affects the bandgap width that shifts toward higher energies, which was also noted in the studies of optical absorption (Fig. 1). Indeed, in the $\sigma(E)$ spectrum of $TiO_2/ZrO_2/SiO_2$ film in the absorption band that corresponds to indirect band-to-band transitions $\Gamma_3 \rightarrow X_{1b}$ and determines the bandgap width, the maximum is located at the energy 3.3 eV, which agrees with the data of optical extinction.

In this case, there is an apparent overlap of the absorption bands with maxima at 2.9 and 3.3 eV. The reason for this overlap may be the presence of surface states (~2.9 eV) and the Urbach tail caused by the nanocrystalline state of TiO_2 anatase. By the way, the surface states may be called forth by adsorption at the interface of nanoparticles belonging to hydroxyl groups of different types. The restructuring of the surface states for various nanocomposites can also lead to a shift of E_{gi} [21].
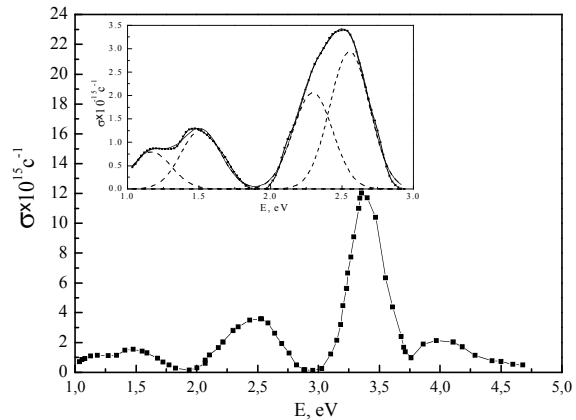

Fig. 6. Spectral dependence of the optical conductivity $\sigma(E)$ for $TiO_2/ZrO_2/SiO_2$ film. (The insert shows decomposition of $\sigma(E)$ into Gaussian components within the range 2.2–3.4 eV.)

So, in TiO_2 and its oxide nanocomposites within the bandgap, there are additional levels that emerge due to the presence of Ti^{3+} ions, Ti interstitial atoms and oxygen vacancies. The probability of electron transitions involving those levels varies depending on the oxide type and contributes to the broadening of the absorption region to the visible range.

Upon adding nanoparticles of silver and gold into the triple system, all absorption centers, characteristic for the triple film, retain except for the F centers. However, the spectral dependence of optical conductivity has some peculiarities. Specifically, as shown in Fig. 7, for $TiO_2/ZrO_2/SiO_2/Ag$ film, as well as for the triple film, the absorption bands corresponding to the F^{2+} color centers and interstitial atoms (i_o(Ti)) retain their positions at 1.2 and 1.5 eV, respectively. The maxima of absorption bands at 2.3 and 2.55 eV correspond to absorption caused by the presence of Ti^{3+} ions and F^+ centers, respectively.

Fig. 5. Spectral dependence of optical conductivity $\sigma(E)$ for the TiO_2/ZrO_2 film. (The insert shows the decomposition of $\sigma(E)$ into Gaussian components within the range 1.4–3.2 eV.)
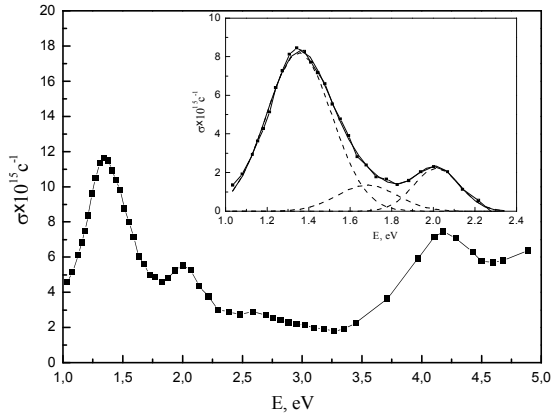

Fig. 7. Spectral dependence of the optical conductivity $\sigma(E)$ for the $TiO_2/ZrO_2/SiO_2/Ag$ film. (The insert shows decomposition of $\sigma(E)$ into Gaussian components within the range 1.0 – 3.0 eV).

Fig. 8. Spectral dependence of the optical conductivity σ(*E*) for the TiO$_2$/ZrO$_2$/SiO$_2$/Au film. The insert shows decomposition of σ(*E*) into Gaussian components within the range 1.0–2.4 eV.

While the spectral dependence of optical conductivity σ$\left(E\right)$ for the triple film containing Ag nanoparticles retains the main features that were ascribed to the binary and ternary films, in the case of adding Au nanoparticles, its behavior changes significantly.

Thus, for TiO$_2$/ZrO$_2$/SiO$_2$/Au film (Fig. 8), there is an absorption band that corresponds to interstitial atoms in octahedral pores i_o(Ti), which shifts toward higher energies and is located at 1.7 eV. For this film, there are also bands of optical conductivity at 2.0 and 2.6 eV that correspond to absorption by Ti^{3+} and F$^+$ centers, respectively.

The substantial difference in the optical conductivity spectrum σ$\left(E\right)$ for TiO$_2$/ZrO$_2$/SiO$_2$/Au film is caused by the emergence of a rather intensive absorption band peaking at 1.35 eV. This band, like to that in the case of other composites, can be explained by the existence of F^{2+} centers in TiO$_2$ films. As a result of the presence of Au nanoparticles that act as electron traps in the triple film, the concentration of F^{2+} centers grows. The reason for this growth is the transport of excited electrons, both free and localized on defective levels, to the Au nanoparticles, which causes an increase in oxygen vacancy content without charge trapping. The absorption band at 4.2 eV corresponds to the existence of a direct transfer, which is consistent with the data for E_{gd} = 4.2 eV, obtained from the intersection of the (α*hν*)^2 tangent with the electron energy axis.

Table 2 gives the energies of electron transitions in TiO$_2$, TiO$_2$/ZrO$_2$, TiO$_2$/ZrO$_2$/SiO$_2$, TiO$_2$/ZrO$_2$/SiO$_2$/Ag, TiO$_2$/ZrO$_2$/SiO$_2$/Au films associated with the existence of intrinsic structural defects in TiO$_2$ and their corresponding values of the optical conductivity σ$\left(E\right)$.

It was noted that the positions of optical conductivity bands in TiO$_2$, TiO$_2$/ZrO$_2$ and

TiO$_2$/ZrO$_2$/SiO$_2$ films doped with noble metals significantly depend on the film composition. Substantial changes were also observed in the values of optical conductivity σ$\left(E\right)$ (Table 2). It is worth noting that a significant increase in the optical conductivity σ$\left(E\right)$ for the triple film TiO$_2$/ZrO$_2$/SiO$_2$ occurs as compared to the individual TiO$_2$ and double TiO$_2$/ZrO$_2$ films.

So, considering the value of optical conductivity associated with absorption by F^{2+} centers, we can see that it is almost the same for TiO$_2$ film and the triple film containing Ag. In the case of binary TiO$_2$/ZrO$_2$ film, the value of optical conductivity associated with F^{2+} centers is the lowest and equals $0.2 \cdot 10^{15} \text{s}^{-1}$. At the same time, the increase of optical conductivity σ$\left(E\right)$ for the mentioned centers is observed in the case of triple films. In the films with Au nanoparticles, the value of optical conductivity σ$\left(E\right)$ equals $8.5 \cdot 10^{15} \text{s}^{-1}$, which corresponds to absorption by F^{2+} centers, and exceeds the values of optical conductivity for all the other composites by several times.

Table 2. Energies of electron transitions in TiO$_2$, TiO$_2$/ZrO$_2$, TiO$_2$/ZrO$_2$/SiO$_2$, TiO$_2$/ZrO$_2$/SiO$_2$/Ag, TiO$_2$/ZrO$_2$/SiO$_2$/Au films associated with the existence of intrinsic structural defects in TiO$_2$, and their corresponding values of the optical conductivity σ(*E*).

Type of nanocomposite	Type of TiO$_2$ intrinsic structural defects	Energy of electron transition, eV	Optical conductivity σ·10^{15} s^{-1}
TiO$_2$	F^{2+}	1.3	0.5
	i_o(Ti)	1.57	0.45
	i_m(Ti)	1.75	0.95
	Ti^{3+}	1.95	0.7
	F	2.7	1.5
TiO$_2$/ZrO$_2$	F^{2+}	1.25	0.2
	i_m(Ti)	1.82	0.5
	Ti^{3+}	2.1	1.5
	F$^+$	2.55	3.0
TiO$_2$/ZrO$_2$/SiO$_2$	F^{2+}	1.2	1.1
	i_o(Ti)	1.5	1.1
	Ti^{3+}	1.7	1.2
	F	2.7	4.3
TiO$_2$/ZrO$_2$/SiO$_2$/Ag	F^{2+}	1.2	0.75
	i_o(Ti)	1.5	1.25
	Ti^{3+}	2.3	2.1
	F$^+$	2.55	3.5
TiO$_2$/ZrO$_2$/SiO$_2$/Au	F^{2+}	1.35	8.1
	i_o(Ti)	1.7	1.3
	Ti^{3+}	2.0	2.1
	F$^+$	2.6	0.5

Considering the values of optical conductivity that is related to interstitial atoms in octahedral pores i_o(Ti), it is worth noting that it is the lowest for the TiO_2 film and equals $0.45 \cdot 10^{15} \, s^{-1}$, while for $TiO_2/ZrO_2/SiO_2$, $TiO_2/ZrO_2/SiO_2/Ag$, and $TiO_2/ZrO_2/SiO_2/Au$ this value reaches $1.1 \cdot 10^{15}$, $1.25 \cdot 10^{15}$, and $1.3 \cdot 10^{15} \, s^{-1}$, respectively. For the binary film, the bands of optical conductivity corresponding to interstitial atoms in octahedral pores i_o(Ti) were not found. But for the binary TiO_2/ZrO_2 film, there occurs optical conductivity caused by absorption by Ti atoms in tetrahedral pores i_m(Ti), although its value is almost two times smaller as compared to TiO_2 film and equals $0.5 \cdot 10^{15} \, s^{-1}$. For other films, the contribution to optical conductivity from i_m(Ti) was not observed.

It is worth noting that for all the films, absorption by Ti^{3+} ions is characteristic. In the case of TiO_2 film, the value of optical conductivity associated with these structural defects is the lowest compared to other films and equals $0.7 \cdot 10^{15} \, s^{-1}$. For the binary and ternary films, optical conductivity related with Ti^{3+} ions equals $1.5 \cdot 10^{15} \, s^{-1}$ and $1.2 \cdot 10^{15} \, s^{-1}$, respectively. Upon adding metal particles into the triple film, σ reaches $2.1 \cdot 10^{15} \, s^{-1}$ for both film types.

Thus, depending on the composition of oxide nanocomposites based on TiO_2 and depending on the type of noble metal nanoparticles, there is a substantial change of type and concentration of intrinsic defects in TiO_2. Their presence substantially affects the processes of photogeneration of charge carriers and their recombination, which can determine the efficiency of photocatalytic activity in film nanocomposites. Besides, we can expect that by using particle irradiation at the energies that provide Frenkel pair generation, we can change the concentration of the above-mentioned defects. This can substantially affect sensibilization of TiO_2 and its composites to visible light.

4. Conclusions

Thin nanocrystalline films of TiO_2, TiO_2/ZrO_2, $TiO_2/ZrO_2/SiO_2$, $TiO_2/ZrO_2/SiO_2/Ag$ and $TiO_2/ZrO_2/SiO_2/Au$ were obtained by using the sol-gel synthesis method. Their bandgap width was determined from the intersection of the $(\alpha h v)^{1/r}$ tangent with the hv axis, on which the energy of photons for two transition types, direct (E_{gd}) and indirect (E_{gi}), was marked. We found that for TiO_2, $E_{gi} = 3.3$ eV, which coincides with the bandgap width for the anatase phase of bulk TiO_2. Addition of zirconium oxide to TiO_2 leads to a decrease in this value down to 2.9 eV, which is related with the presence of surface levels at the bottom of the conduction band. For the triple films modified with gold and silver nanoparticles, the corresponding bandgap widths are $E_{gi} = 3.6$ eV and $E_{gd} = 4.2$ eV, respectively. These values are substantially overestimated for bandgap widths and correspond to direct transitions with the energies higher than the bandgap width of anatase TiO_2.

It is shown that, depending on the composition of nanocomposites, optical conductivity $\sigma(E)$ has a different character. This is caused by the existence of intrinsic structural defects, namely: oxygen vacancies, Ti^{3+} ions, and interstitial atoms of Ti. Depending on the concentration of mentioned defects, the value of optical conductivity $\sigma(E)$ corresponding to electron transitions related with these structural defects changes, too. The most substantial is the change in the concentration of F^{2+} centers. In particular, it has the highest value for triple films with gold nanoparticles.

Upon the restructuring of the energy spectra, especially within the bandgap, we can expect a substantial change in photogenerative and recombinational properties of TiO_2 thin films, which leads to the improvement of photocatalytic activity in the UV and visible ranges.

References

1. H. Tang, H. Berger, P.E. Schmid, F. Levy, G. Burri, Photoluminescence in TiO_2 anatase single crystals // *Solid State Communs.* **87**(9), p. 847-850 (1993).
2. M. Andrulevicius, S. Tamulevicius, Yu. Gnatyuk, N. Vityuk, N. Smirnova, A. Eremenko, XPS investigation of $TiO_2/ZrO_2/SiO_2$ films modified with Ag/Au nanoparticles // *Mater. Sci.* **14**(1), p. 8-14 (2008).
3. A.A. Lisachenko, R.V. Mikhailov, Point defects as the centers of titanium dioxide sensitization in the visible spectral range // *Technical Phys. Lett.* **31**(1), p. 42-49 (2005).
4. R.F. Hairutdinov, Chemistry of semiconductor nanoparticles // *Uspekhi khimii*, **67**(2), p. 125-139 (1998), in Russian.
5. H. Luo, T. Takata, Y. Lee, K. Domen, J. Zhao, Y. Yan, Photocatalytic activity enhancing for titanium dioxide by co-doping with bromine and chlorine // *Chem. Mater.*, **16**, p. 846-849 (2004).
6. F. Gonella, G. Mattei, P. Mazzoldi, G. Battaglin, A. Quaranta, G. De, M. Montecchi, Structural and optical properties of silver-doped zirconia and mixed zirconia-silica matrices obtained by sol-gel processing // *Chem. Mater.*, **11**, p. 814-821 (1999).
7. M.D. Hermandez-Alonso, I. Tejedor-Tejedor, J.M. Coronado, J. Soria, M.A. Anderson, Sol-gel preparation of TiO_2–ZrO_2 thin films supported on glass rings: Influence of phase composition on photocatalic activity // *Thin Solid Films*, **502**, p. 125-131 (2006).
8. N. Vituk, Ya. Divinskiy, G. Yeremenko, N. Smirnova, O. Oranska, Sol-gel synthesis of TiO_2/ZrO_2 film for photocatalytic recovery of Cr(VI) in water environment // *Chemistry, physics and technology of surface*, **9**, p. 76-81 (2003), in Ukrainian.

9. L. Byung-Yong, P. Sang-Hyuk, K. Misook, L. Sung-Chul, C. Suk-Jin, Preparation of Al/TiO$_2$ nanometer photocatalyst film and the effect of H$_2$O addition on photo-catalytic performance for benzene removal // *Appl. Catal. A: General*, **253**, p. 371-380 (2003).

10. M.E. Zorn, D.T. Tompkins, W.A. Zelter, M.A. Anderson, Catalytic and photocatalytic oxidation of ethylene on titania-based thin films // *Environ. Sci. Technol.*, **34**, p. 5206-5210 (2000).

11. W. Choi, A. Termin, M.R. Hoffmann, The role of metal ion dopants in quantum-sized TiO$_2$: Correlation between photoreactivity and charge carrier recombination dynamics // *J. Phys. Chem.*, **98**, p. 13669-13679 (1994).

12. V. Subramanian, E. Wolf, P.V. Kamat, Semiconductor-metal composite nanostructures. To what extent do metal nanoparticles improve the photocatalytic activity of TiO$_2$ films? // *J. Phys. Chem. B*, **105**, p. 11439-11446 (2001).

13. T.O. Busko, O.P. Dmitrenko, N.P. Kulish, N.M. Beliy, N.V. Vituk, A.M. Yeremenko, N.P. Smirnova, V.V. Shalackaya, Optical properties of radiationally sensitized TiO$_2$ films with anatase structure // *Voprosy atomnoi nauki i tekhniki*, **2**, p. 32-36 (2008), in Russian.

14. N. Serpone, D. Lawless, R. Khairutdinov, Size effects on the photophysical properties of colloidal anatase TiO$_2$ particles: Size quantization or direct transitions in this indirect semiconductor? // *J. Phys. Chem.*, **99**, p. 16646-16654 (1995).

15. A.L. Stroyuk, A.I. Krukov, S.Ya. Kuchmiy, V.D. Pokhodenko, Quantum size effects in the photonics of semiconductor nanoparticles // *Theoretical and experimental chemistry,* **41**(2), p. 67-91 (2005).

16. Yu.I. Gnatuk, Ye.V. Manuilov, N.P. Smirnova, G.M. Yeremenko, Synthesis, structure and optical characteristics of TiO$_2$/Ag films active during photooxidation of radomin B // *Fizika I khimia tverdogo tela,* **7**, №1 p. 107-112 (2006), in Russian.

17. J. Nowotny, T. Bak, M.K. Nowotny, L.R. Sheppard, TiO$_2$ surface active sites for water splitting // *J. Phys. Chem. B*, **110**, p. 18492-18495 (2006).

18. V.S. Staschuk, R.I. Khamikov, O.P. Polyanska, Influence of structure transformations on optical properties of thin films of cobalt // *Bulletin of Taras Shevchenko National University of Kyiv.* Series: Phys. and Math. Sci. **2**, p. 45-50 (2009).

19. A.A. Lisachenko, V.N. Kuznetsov, M.N. Zakharov, R.V. Mikhailov, An interaction of O$_2$, NO, N$_2$O with surface defects of dispersive titanium dioxide // *Kinetics and Catalisys*, **45** (2), p. 205-213 (2004).